KERNFORSCHUNGSZENTRUM

KARLSRUHE

April 1970

KFK 1157
IAEA-SM-130/41

Institut für Reaktorentwicklung
Projekt Schneller Brüter

Flow Induced Temperature and Pressure Pulsations in Rod Bundles

J. Kadlec, W. Lang

GESELLSCHAFT FÜR KERNFORSCHUNG M. B. H.

KARLSRUHE

KERNFORSCHUNGSZENTRUM KARLSRUHE

April 1970

KFK 1157

IAEA-SM-130/41

Institut für Reaktorentwicklung

Projekt Schneller Brüter

FLOW INDUCED TEMPERATURE AND PRESSURE PULSATIONS IN ROD BUNDLES

J.Kadlec

W.Lang

Gesellschaft für Kernforschung mbH.,Karlsruhe

Abstract

Experiments are described, which are carried out to investigate the random pressure and temperature pulsations of a coolant flow and their consequences. Water circuit experiments with a fuel subassembly provided an indication of the correlation between pressure fluctuations and vibrations of the fuel pins. The temperature pulsations were investigated in a sodium loop. A description is given of the test facilities and the test results.

Zusammenfassung

Es wird über Experimente berichtet, welche zur Untersuchung der in einer Kühlmittelströmung auftretenden stochastischen Druck- und Temperaturpulsationen und deren Auswirkungen durchgeführt wurden. Wasserkreislaufversuche mit einem Brennstabbündel ergaben eine Aussage über die zwischen Druckpulsationen und Brennstabschwingungen bestehende Korrelation. Die Temperaturpulsationen wurden an einem Natriumkreislauf untersucht. Die Versuchseinrichtungen und die Versuchsergebnisse werden beschrieben.

INTERNATIONAL ATOMIC ENERGY AGENCY

SYMPOSIUM ON PROGRESS IN SODIUM-COOLED FAST REACTOR ENGINEERING

March 23 - 27, 1970

M o n a c o

IAEA-SM-130/41

FLOW INDUCED TEMPERATURE AND PRESSURE PULSATIONS IN ROD BUNDLES

J. Kadlec
W. Lang

Nuclear Research Center Karlsruhe,
Federal Republic of Germany

The submitted paper deals with the turbulent pressure and temperature fluctuations in the coolant flow, investigated within the framework of the fast breeder reactor development program in the Institute of Reactor Development of the Karlsruhe Nuclear Research Center. Both processes are treated as inputs of other random processes - vibrations of fuel rods and thermal stresses in core components. Because of this, spectral density functions of both inputs and outputs as well as the frequency response functions of the responding components are of primary interest.

The measurements of the boundary layer pressure fluctuations have been carried out using the mock-up of the fuel subassembly of the 1.000 MW fast reactor design Na 1 /1/. (The subassembly mock-up was mounted in a simple water test-loop, described in detail in report /2/.) The bundle of this mock-up (Fig. 1) has 37 pins, 6.7 mm OD, 2.676 mm length. The pins are supported on 8 locations by the spacer grids illustrated in Fig. 2. These spacer grids as well as other obstacles in the coolant flow are causing relatively high leveled pressure fluctuations. The pressure fluctuations at the wall beneath the turbulent boundary layer have been measured with the Culite miniature pressure transducers (membrane diameter 1.8 mm), flush-mounted in several locations (locations I, A-Z, ALPHA and V - s. Fig. 1) on the hexagonal subassembly sheath and in one location on one of the pins (Fig. 3). In addition to this, three other pins were instrumented with 8 strain gauges each for the measurement of the bending strains of the lateral vibrating pins. The strain gauges were mounted in two different cross sections in the gas plenum inside the pin. There were two strain gauge-half-bridges in each of these two cross sections. The locations of the strain gauges and of the pressure transducers in cross section A of the bundle are given in Fig. 3.

The strain gauges as well as the pressure transducers are connected to the data acquisition system illustrated in Fig. 4. The amplified signals from the transducers are sampled, converted into 11- bit words and written in IBM computer format on the magnetic tape. The processing of the data is carried out separately on IBM 360/65; the results are the auto- and cross-correlation functions and the corresponding spectral densities. Using the described arrangement the systematical study of the boundary layer pressure fluctuations is carried out; some preliminary results from these investigations will be presented here.

The RMS-values $\sqrt{\overline{p^2}}$ of the boundary layer pressure fluctuations, divided by the corresponding mean value of the dynamic pressure q of the flowing water are plotted as a function of the Reynolds Number Re; a typical result of this type is presented in Fig. 5 (pressure transducer D). The mentioned form of the $\sqrt{\overline{p^2}}/q$-Re dependence is typical for the whole pressure field. For higher Reynolds Numbers the measured pressure fluctuations approach a constant value which differs from one location of the transducer to another. The profile of the pressure field between two adjacent spacer grids is illustrated in Fig. 6. The values of the pressure fluctuations increase steeply immediately after the grid, reach a maximum value approximately after three hydraulic diameters and fall again. A similar dependance on the coordinate had been observed also for the local heat transfer coefficients /3/, /4/. Because of difficulties connected with the measurement of the local heat transfer and relative easy way of measuring the pressure fluctuations, it seems justifiable to study the correlation between the local heat transfer and the fluctuating turbulent pressure field in more detail. The spectral density functions in Fig. 7 illustrate how the energy content of the vortexes in fluid changes with the dimensionless coordinate x/d_H. The vortexes with high energy content in a high frequency band are induced immediately after the grid and diminish with the coordinate. The medium frequency vortexes, which causes increase of the local heat transfer coefficient, have maximum energy contents at the coordinate $x/d_H = 3$, where the maximum heat transfer could be expected. For high values of dimensionless coordinate x/d_H the spectral density curve converges to the exponential form.

Another correlation exists between the fluctuating pressure field and the lateral vibration of the fuel pins. The dependance of the RMS values of the vibration amplitude, divided by the mean dynamic pressure of the flowing media, on the Reynolds Number, is similar to that given in Fig. 5 /5/. The correlation between the turbulent pressure field and the vibrating response of the pin is illustrated in Fig. 8. Two diagrams in the center of the figure depict the spectral density functions of the strain of the vibrating pin No. VI measured in two perpendicular directions y and z (Fig. 3). The adjacent diagrams above and below depict the corresponding spectral density functions of the pressure fluctuations at the wall opposite the pin (pressure transducer on the pin for the measurement of the normal pressure in direction y, pressure transducer in the subassembly wall for direction z - Fig. 3). The coincidence of the frequency bands for both pressure fluctuation and pin vibration is demonstrated in these diagrams.

Analytical formulation of the dependance of the fuel rod vibration on the random pressure forces of the coolant is described in terms of spectral density functions in the following equation /5/:

$$S_y(x,\omega) = \sum_{j=1}^{\infty} \sum_{k=1}^{\infty} \frac{G_j(x) \cdot G_k(x)}{Z_j(\omega) \cdot Z_k(-\omega)} S_{\phi jk} \tag{1}$$

where

$$S_{\phi jk} = \int_0^l \int_0^l G_j(\xi_1) \cdot G_k(\xi_2) \cdot S_f(\xi_1, \xi_2, \omega)\, d\xi_1\, d\xi_2 \tag{2}$$

and

$S_y(x,\omega)$ is the spectral density function of the vibration displacement y,

$S_f(x_1,x_2,\omega)$ is the cross-spectral density function of the random coolant forces,

$G_j(x)$ is the normal function of the j-th vibration mode,

$Z_j(\omega)$ is the modal impedance,

x, l and $\omega = 2\pi\nu$ describe the coordinate, fuel rod length and angular frequency, respectively.

The methods for investigating the functions $G_j(x)$, $Z_j(\omega)$ and $S_y(x,\omega)$ are presented in reports /6/, /7/ and /2/. Current work has the object to describe the cross-spectral density function $S_f(x_1,x_2;\omega)$. At present measures are taken to reduce the influence of the machinary noise of the loop upon the fluctuating pressure field in the bundle. It is expected that subsequent measurements will bring more detailed information about the subject discussed.

The turbulent temperature fluctuations in sodium were measured under the condition of an intensive heat transfer from the heated wall to the flowing coolant. The test section is illustrated in Fig. 9; a detailed description of the sodium loop is given in /8/. The nickel tube, 8.5 mm ID, was heated by induction over a length of 165 mm. The temperature fluctuations in sodium were detected by four Ni-NiCr thermocouples, 0,5 mm OD of sheath. The thermocouples were mounted in a row on the outlet side of the test section. The first thermocouple No. 14 is located 30 mm after the end of the heated zone, the spacing of the following thermocouples Nos. 13 to 11 in a row is 4 mm. The calculated frequency response function $H(\nu)$ of these thermocouples is given in Fig. 10. From the diagram follows that the measured spectral density function of the temperature fluctuations must be corrected for $\nu > 3$ Hz. The parallel of the input-output relation (1) for this case reads /9/

$$S_{t\,meas}(\nu) = \left|H(\nu)\right|^2 S_{treal}(\nu), \tag{3}$$

where $S_{tmeas}(\nu)$ and $S_{treal}(\nu)$ indicate measured and real spectral density functions of the temperature fluctuations, respectively. The measured spectral density function of all 4 thermocouples for the heat flow Q=584 W/cm² (w = 3,34 m/sec, Re = 104,000, sodium mean temperature $\bar{t}$ = 483 °C) is given in Fig. 11. The curves in the diagrams have similar forms to the spectral density functions of pressure fluctuations in Fig. 7, and a similar tendency of a change with the coordinate takes place. As in the case of pressure fluctuations, the spectral analysis of temperature fluctuations seems to be a promissible tool for the study of the flow structure.

In case the coolant gets into contact with the structure, temperature fluctuations in the coolant cause thermal stresses in reactor components. If the spectral density function $S_t(\nu)$ of the temperature fluctuations is known, the corresponding spectral density function of the thermal stresses $S_\sigma(\nu)$ of the responding component can be determined in accordance with equation

$$S_\sigma(\nu) = \left|H_{\sigma t}(\nu)\right|^2 S_t(\nu) \tag{4}$$

The function

$$H_{\sigma t}(\nu) = \left|H_{\sigma t}(\nu)\right| \cdot e^{-j\varnothing(\nu)} \tag{5}$$

is the frequency response function of the component; $\varnothing(\nu)$ is a phase shift /9/.

As an example, the frequency response function of a simple component will be demonstrated. The investigated component which is typical for core design is illustrated in Fig. 12. A hollow cylinder (ID 100 mm, OD 104 mm) with a thick walled ring (OD 140 mm) was instrumented with thermocouples (Ni-NiCr thermocouples 0,5 mm OD of sheath), temperature sensor gauges (STG 50,Micro-Measurements) and temperature compensated strain gauges (SK-09-062, Micro-Measurements). The material of the test component is stainless steel X8CrNiNb 1613. The frequency response functions for the temperature and strain field of the component were determined by measuring input and output signals during the temperature cycling tests in a helium loop described in /10/. As an example, the frequency response function $H_{\varepsilon t}(\nu)$ of the strain ε, for the strain gauge location D5 is given in Fig. 13. The tests were performed with a helium mass flow of 150 kg/h and a static pressure of 8 kp/cm^2; the helium temperature was varied periodically at different frequencies in the range 50 to 180 °C. An interesting phenomena of the frequency response function in Fig. 13 is the occurrence of two maxima. The maximum at low frequency ($3 \cdot 10^{-3}$ Hz) corresponds to the bending stresses induced by the different temperature of the thick and thin walled parts of the test component. The second maximum ($5 \cdot 10^{-2}$ Hz) is due to the thermal stress induced by the radial temperature gradient in the wall (skin stress). Both peaks are inside the frequency range where the spectral density function of the temperature fluctuations reaches its maximum value. In the case of sodium coolant the frequency response function rises approximately at linear rate with the rise of the heat transfer coefficient.

The investigations of temperature fluctuations in sodium are continued. At present, the data of the measurement of the correlated temperature fluctuations in sodium flow are processed.

REFERENCES

/1/ SMIDT, D., MÜLLER, A., Referenzstudie für den 1000 MWe natriumgekühlten schnellen Brutreaktor (Na 1), KFK 299, Kernforschungszentrum Karlsruhe, Dezember 1964.

/2/ KADLEC, J., APPELT, K.D., Methode für die experimentelle Untersuchung des durch die Kühlmittelströmung hervorgerufenen Schwingungszustandes der Brennstäbe, KFK 1082, Kernforschungszentrum Karlsruhe, November 1969, in press.

/3/ Experimental Investigations of Heat Transfer and Fluid Flow, Part 1.3, ORNL-Report 2888, December 1959.

/4/ VLČEK, J., WEBER, P., Experimentální výzkum lokálního součinitele přestupu tepla v oblasti distančních buněk palivového článku, Jaderná energie 14 , 12 (1968), 419-425.

/5/ KADLEC, J., Allgemeine Betrachtung über die durch die Kühlmittelströmung hervorgerufenen Schwingungen der Brennstoffstäbe des schnellen Brutreaktors 1000 MW, Ext. Bericht 8/66-5, Kernforschungszentrum Karlsruhe, Dezember 1966.

/6/ KADLEC, J., Rechnungsverfahren für die Bestimmung der Eigenfrequenzen, der Normalfunktionen und der Dehnungsfunktionen querschwingender Brennstäbe, Ext. Bericht 8/66-9, Kernforschungszentrum Karlsruhe, September 1966.

/7/ KADLEC, J., PFROMMER, V., Methode für die experimentelle Untersuchung der Eigenfrequenzen, der Normal- und der Dehnungsfunktionen sowie der Dämpfung der querschwingenden Brennstäbe, KFK 731, Kernforschungszentrum Karlsruhe, März 1968.

/8/ PEPPLER, W., "Natrium-Siedestoßexperimente in einem größeren Kreislauf unter Verwendung induktiv beheizter Teststrecken", Zur Entwicklung schneller Brutreaktoren, KFK 964, Kernforschungszentrum Karlsruhe, April 1969.

/9/ LANG, W., Ein Beitrag zur experimentellen Thermoschockanalyse, Ext. Bericht 8/69-3, Kernforschungszentrum Karlsruhe, Mai 1969.

/10/ LANG, W., Eine Methode zur experimentellen Thermoschockanalyse, KFK 1168, Kernforschungszentrum Karlsruhe, April 1970

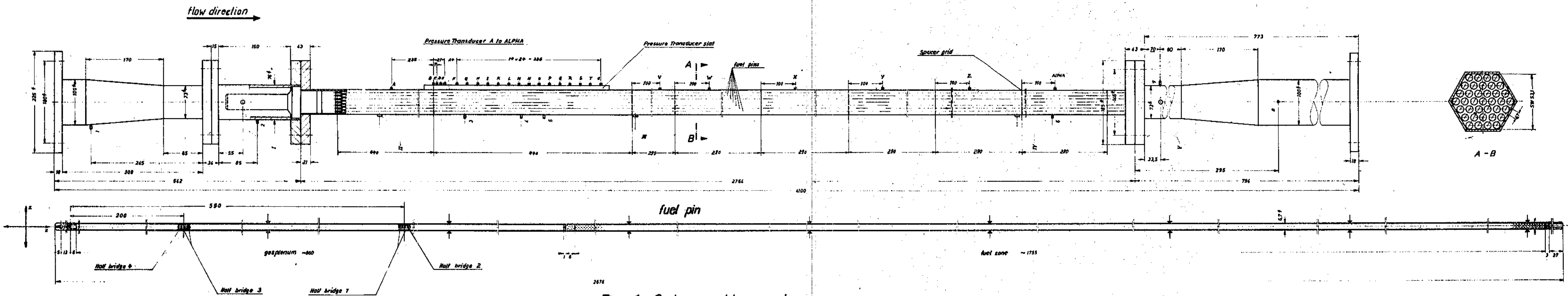

Fig.: 1 Subassembly mock-up

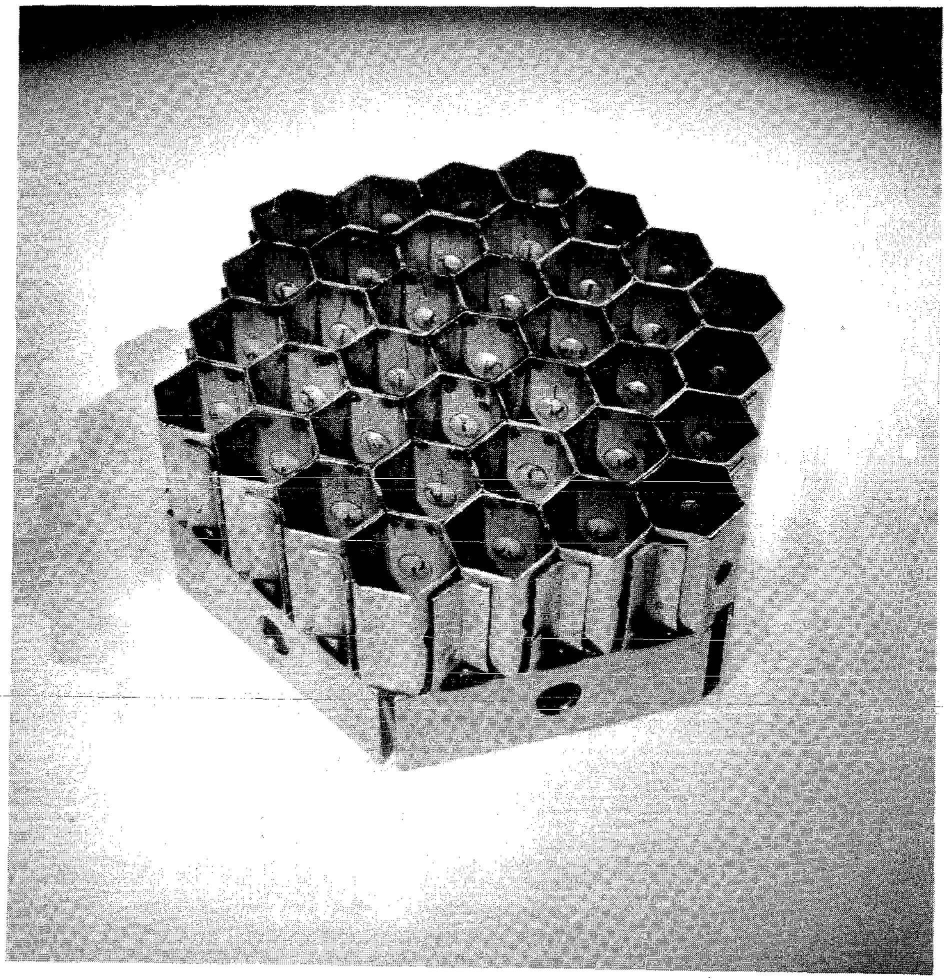

Fig. 2: Spacer grid

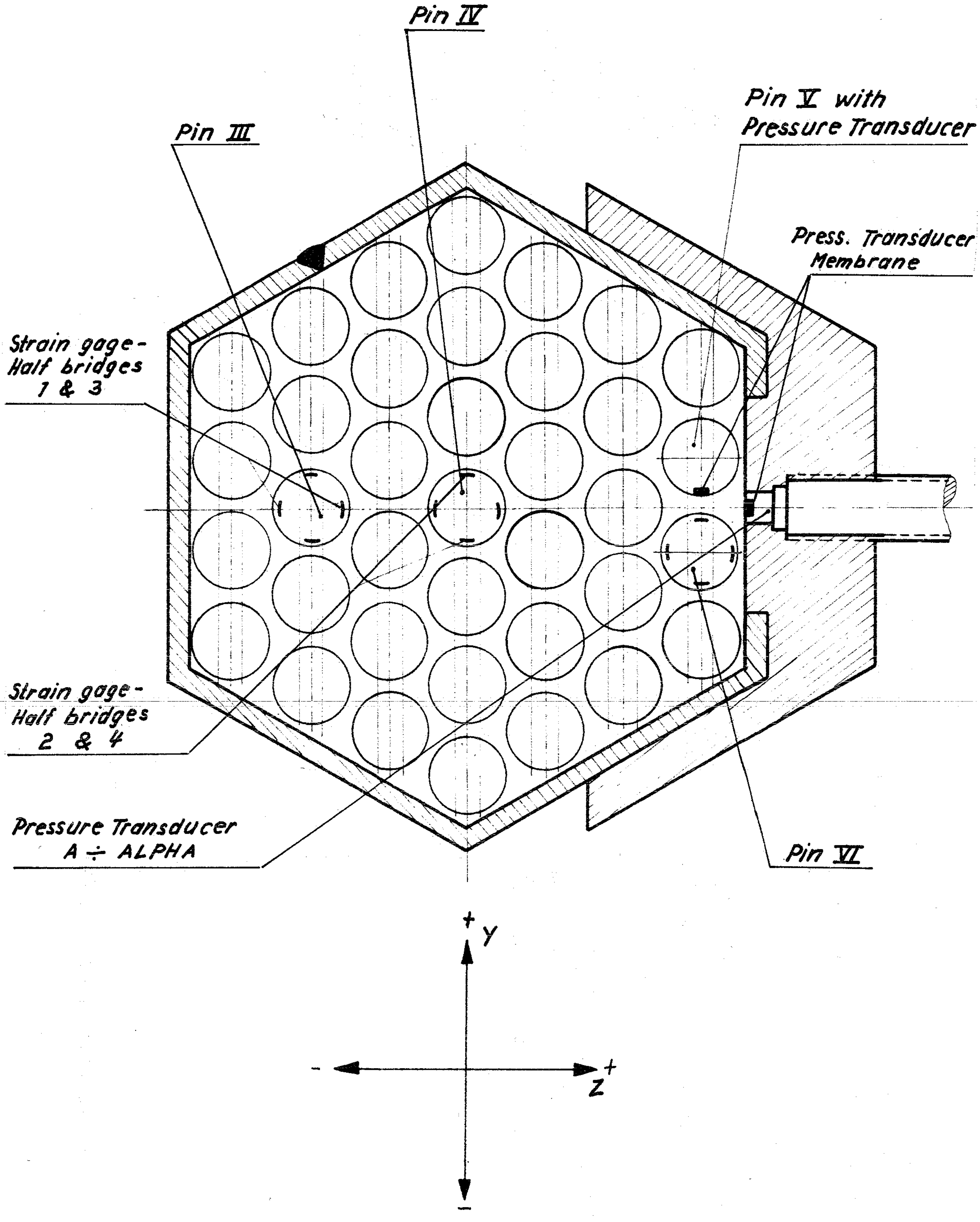

Fig.: 3 Location of transducers

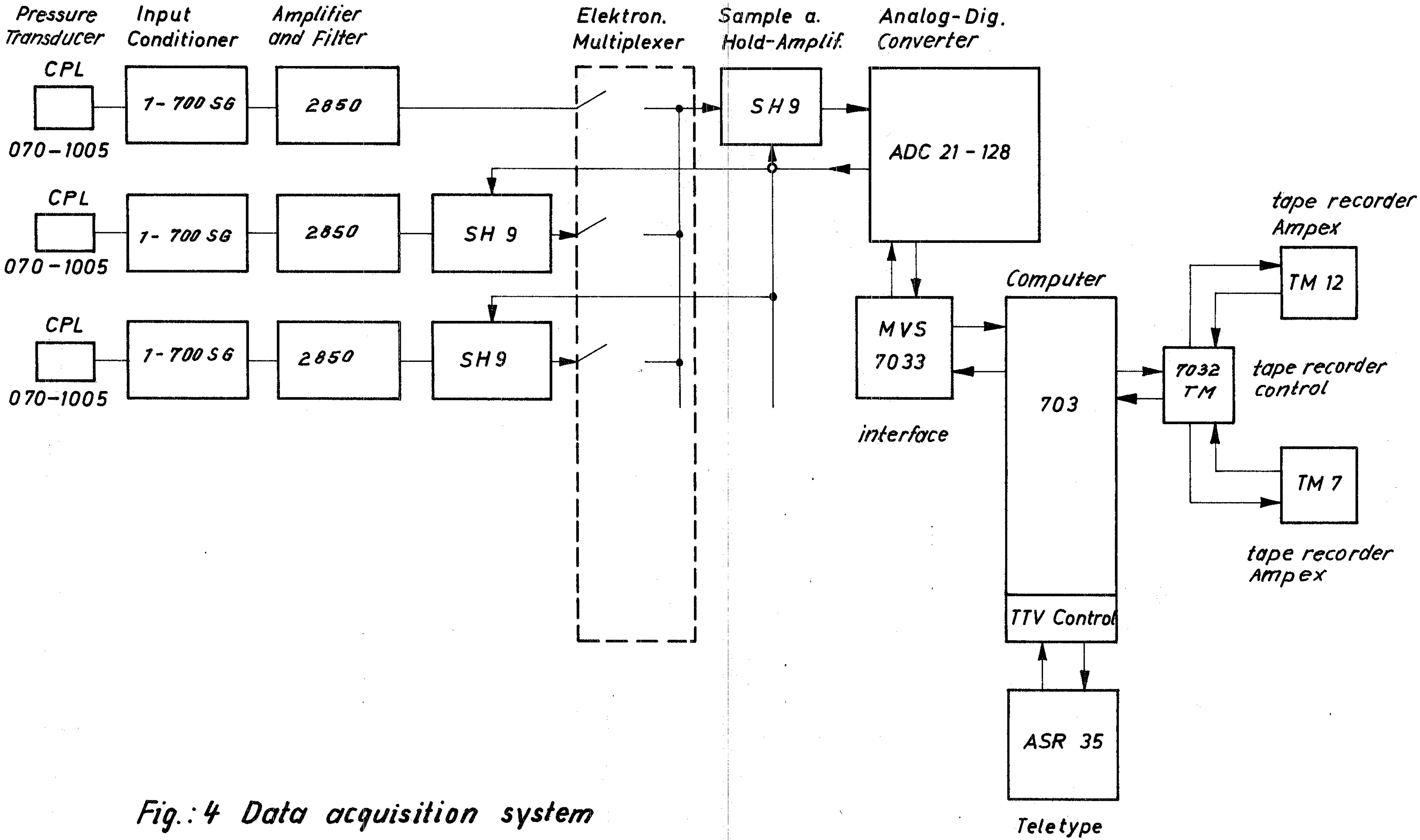

Fig.: 4 Data acquisition system

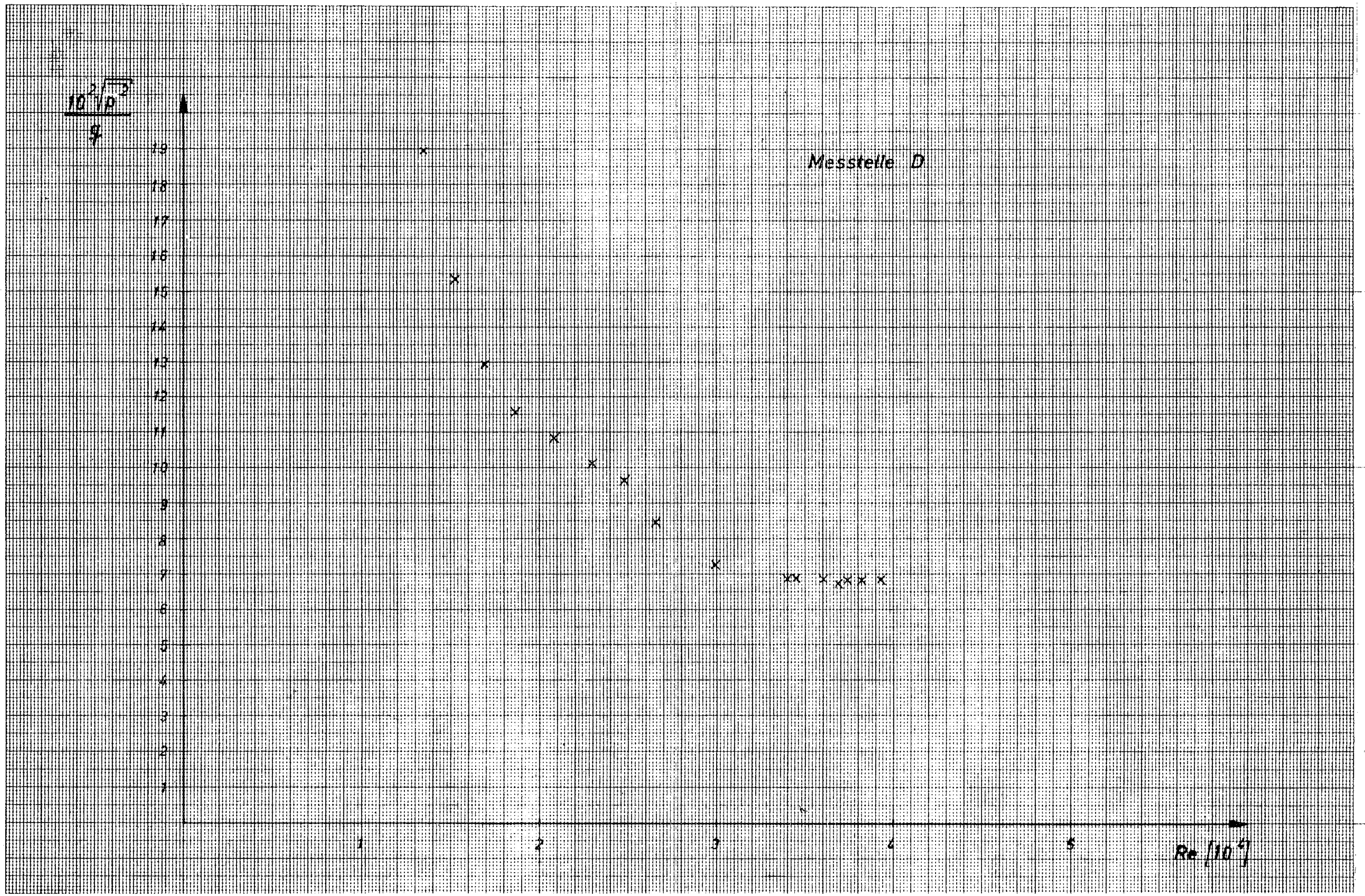

Fig.: 5 RMS - pressure fluctations

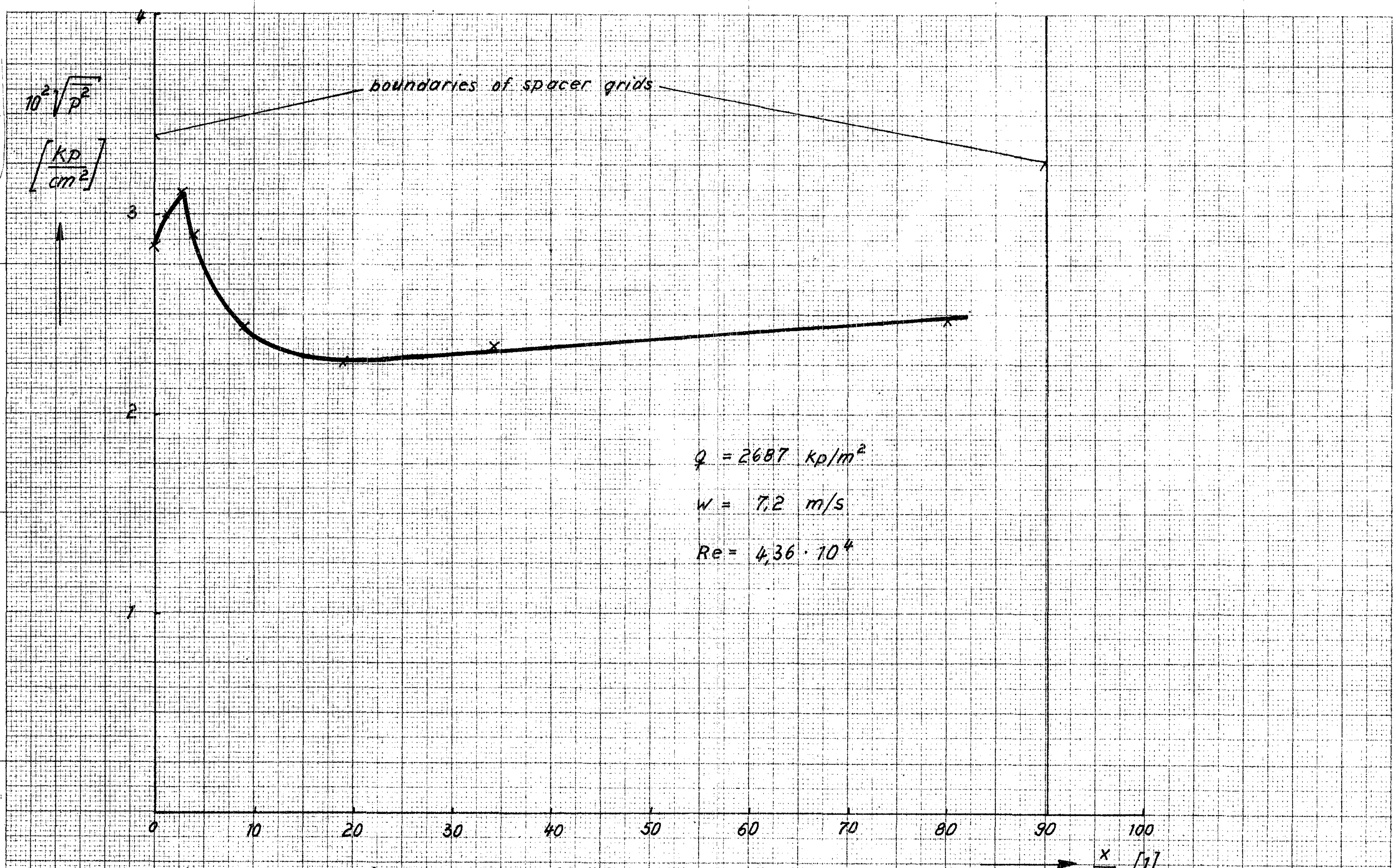

Fig.: 6 Fluctuating pressure field

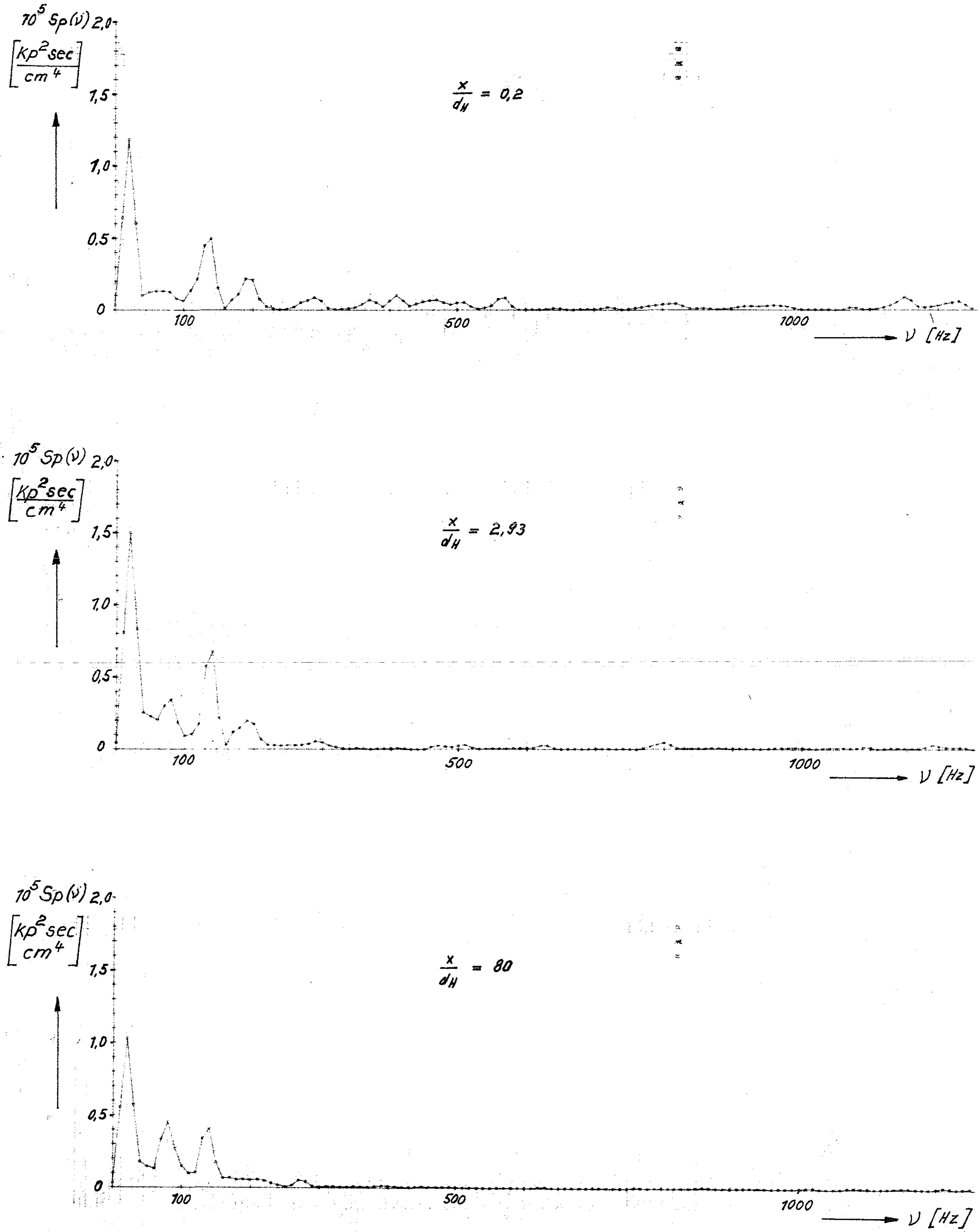

Fig.: 7 Dependance of $S_p(\nu)$ on coordinate $\frac{x}{d_H}$

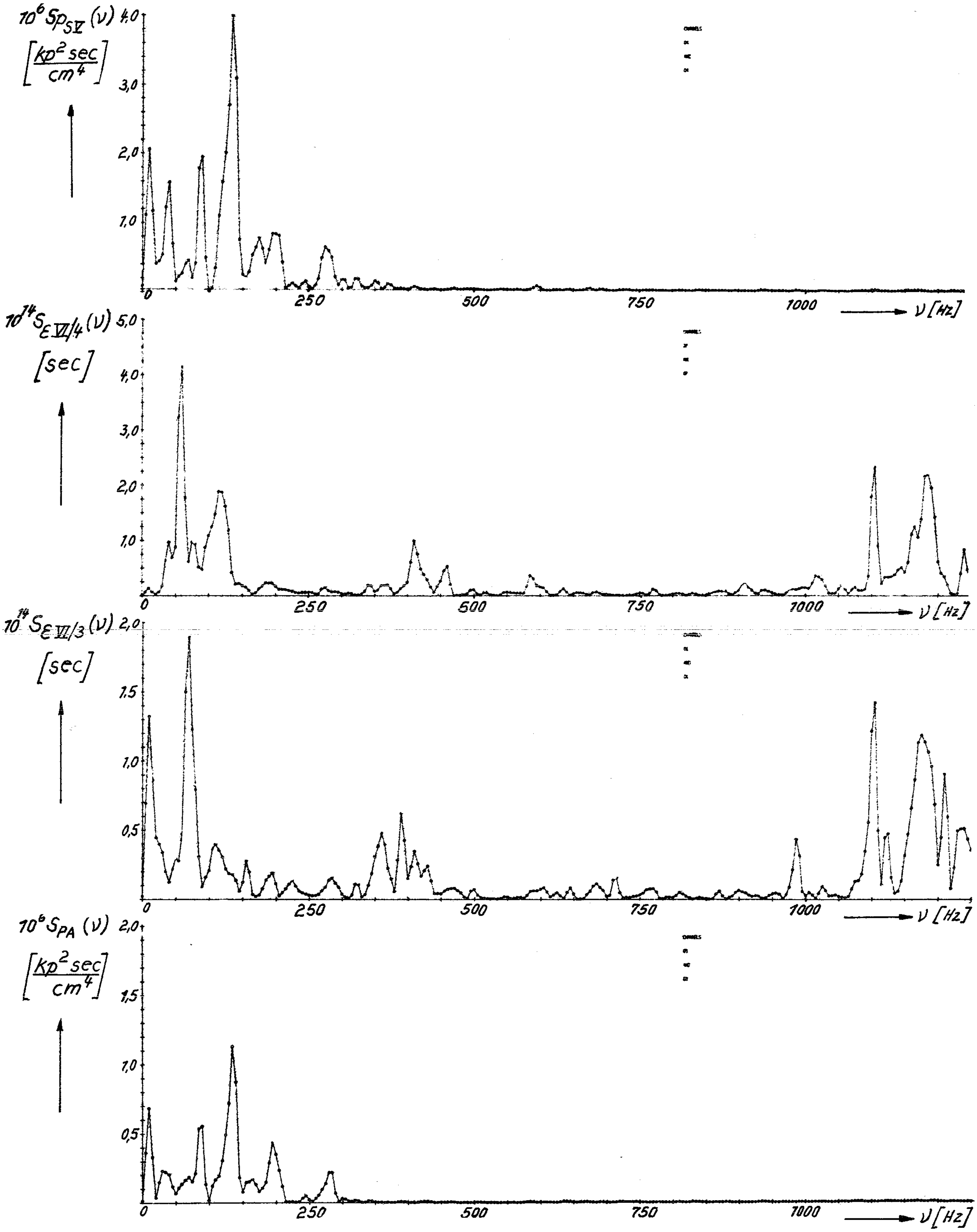

Fig.: 8 Spectral density functions $S_p(\nu)$ and $S_\varepsilon(\nu)$

Liste der Thermoelemente

Nr.	1-3	4-8	9-10	11-14
Φ (mm)	1	0,5	1	0,5
Art	T.M.	T.M.	T.I.	

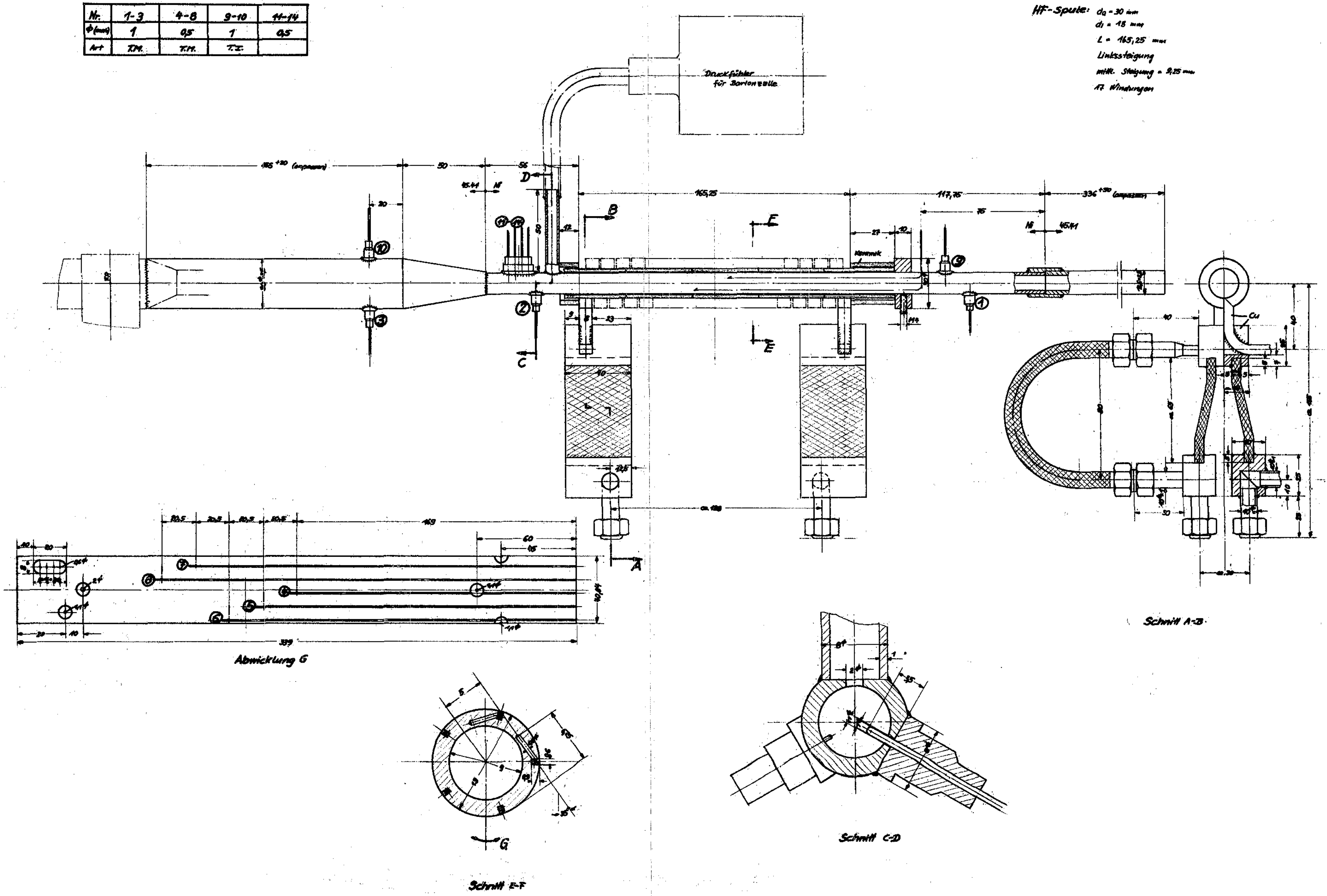

Fig.: 3 Test section for heat transfer in sodium

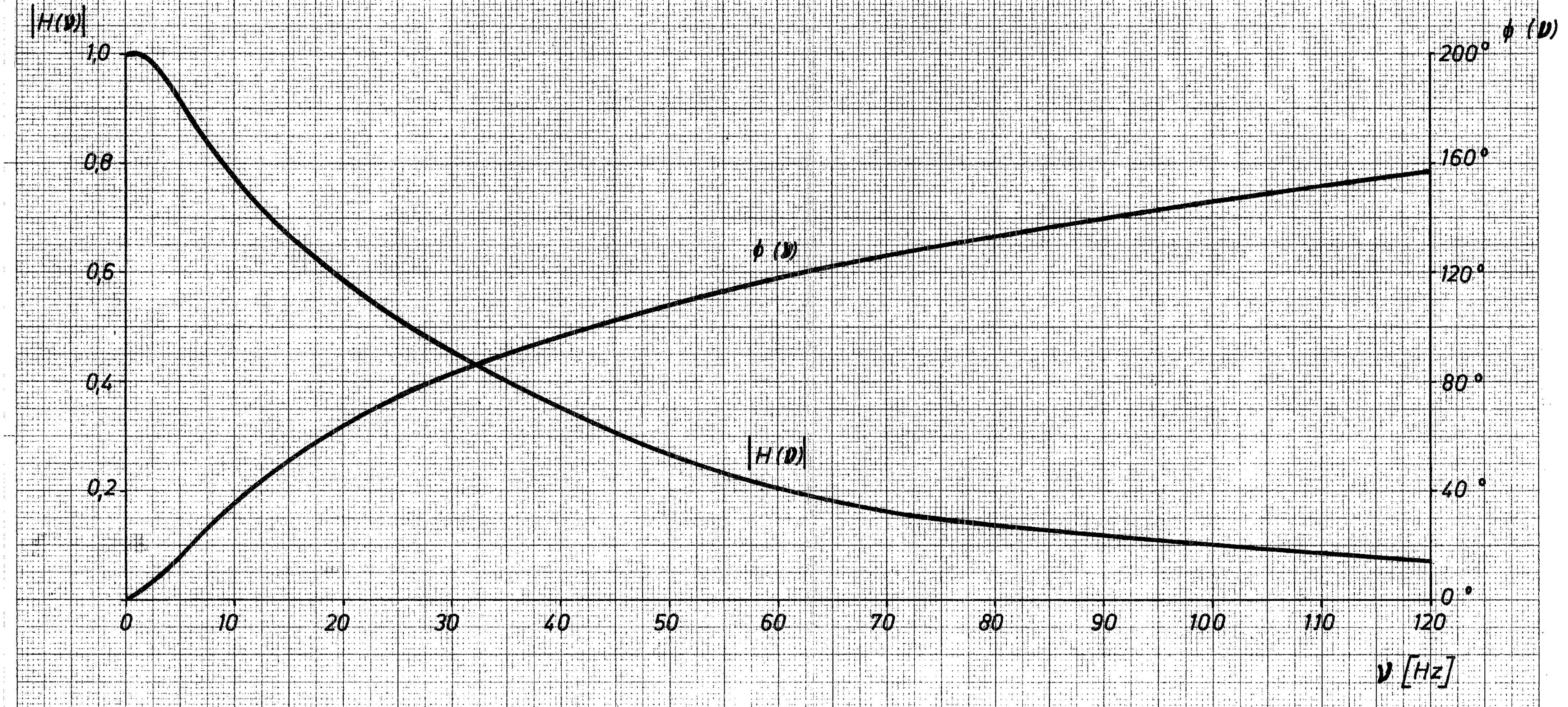

Fig.: 10 Frequency response function of the thermocouple

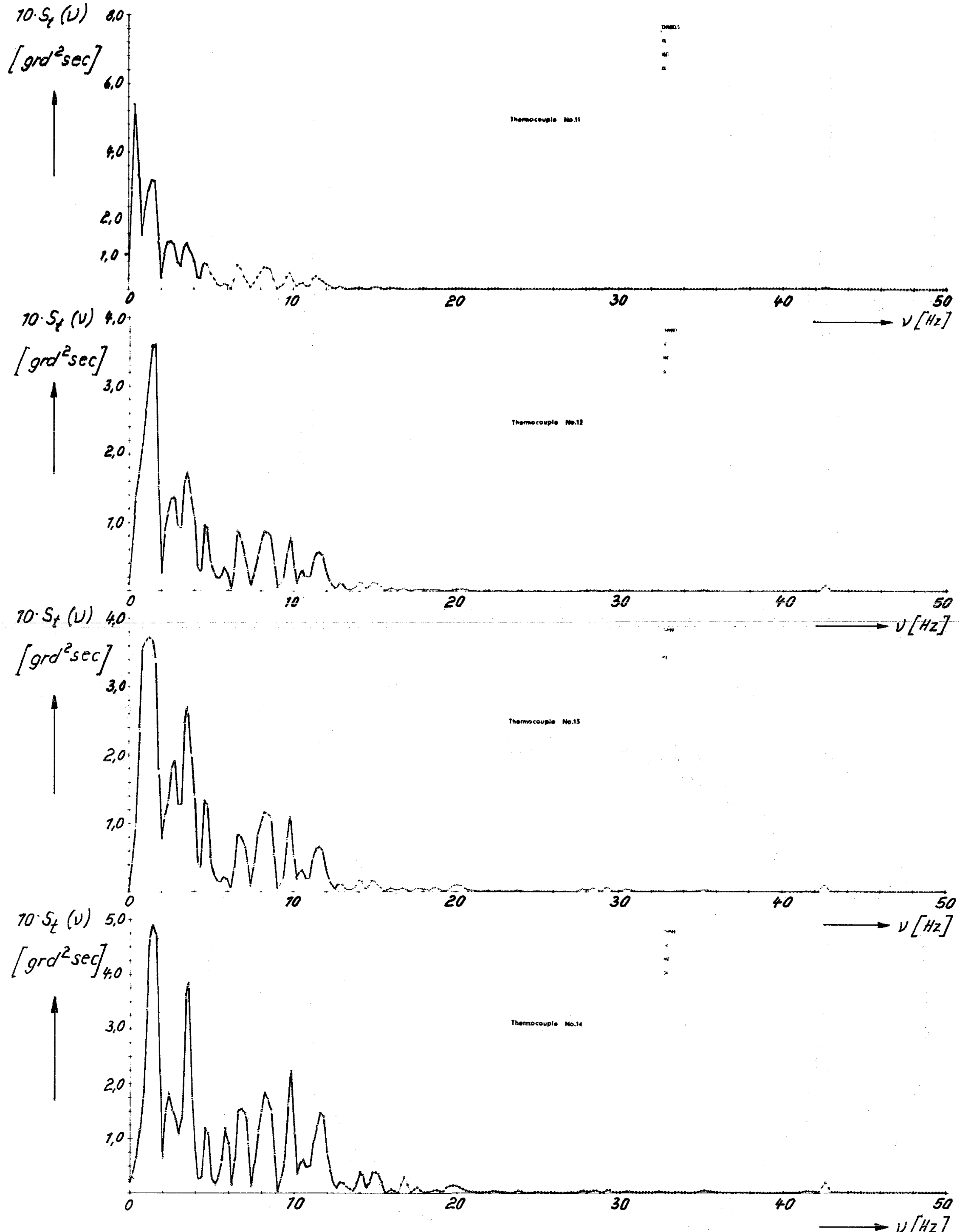

Fig.: 11 Spectral density functions $S_t(\nu)$

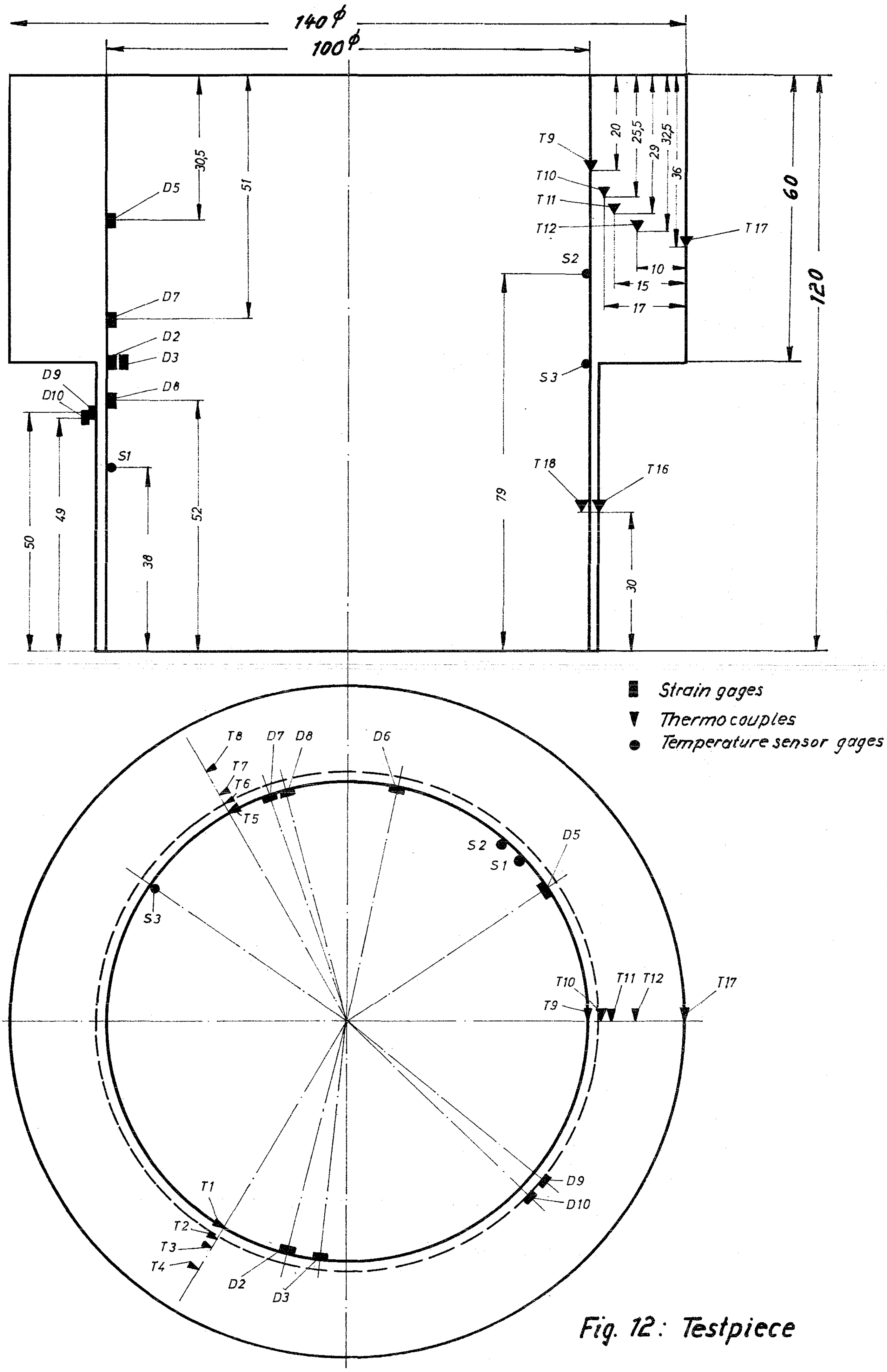

Fig. 12: Testpiece

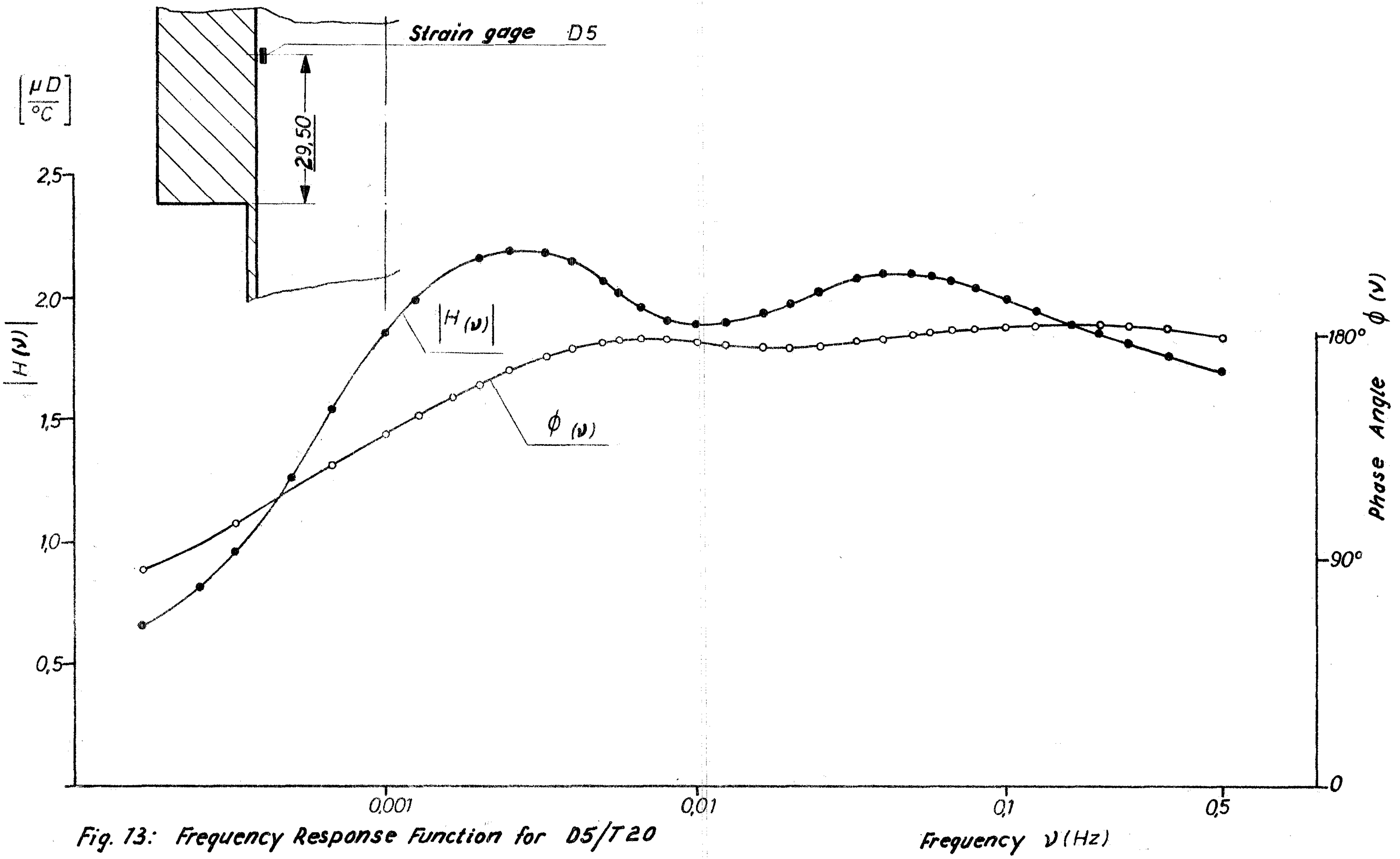

Fig. 13: Frequency Response Function for D5/T20